Molecular Biology of the Cell
Vol. 14, 5028–5037, December 2003

Two Phases of Actin Polymerization Display Different Dependencies on PI(3,4,5)P_3 Accumulation and Have Unique Roles during Chemotaxis

Lingfeng Chen, Chris Janetopoulos, Yi Elaine Huang, Miho Iijima, Jane Borleis, and Peter N. Devreotes*

Department of Cell Biology, Johns Hopkins University, School of Medicine, Baltimore, Maryland 21205

Submitted May 28, 2003; Revised October 7, 2003; Accepted October 10, 2003
Monitoring Editor: Mary Beckerle

The directional movement of cells in chemoattractant gradients requires sophisticated control of the actin cytoskeleton. Uniform exposure of *Dictyostelium discoideum* amoebae as well as mammalian leukocytes to chemoattractant triggers two phases of actin polymerization. In the initial rapid phase, motility stops and the cell rounds up. During the second slow phase, pseudopodia are extended from local regions of the cell perimeter. These responses are highly correlated with temporal and spatial accumulations of PI(3,4,5)P_3/PI(3,4)P_2 reflected by the translocation of specific PH domains to the membrane. The slower phase of PI accumulation and actin polymerization is more prominent in less differentiated, unpolarized cells, is selectively increased by disruption of PTEN, and is relatively more sensitive to perturbations of PI3K. Optimal levels of the second responses allow the cell to respond rapidly to switches in gradient direction by extending lateral pseudopods. Consequently, PI3K inhibitors impair chemotaxis in wild-type cells but partially restore polarity and chemotactic response in *pten*$^-$ cells. Surprisingly, the fast phase of PI(3,4,5)P_3 accumulation and actin polymerization, which is relatively resistant to PI3K inhibition, can support inefficient but reasonably accurate chemotaxis.

INTRODUCTION

A wide variety of cells can carry out chemotaxis or directional movement in response to chemotactic signals. Migration toward a chemoattractant or away from a repellent requires both directional sensing, polarity, and coordinated movement. A cell detects a shallow external gradient and relays the amplified signal to the cytoskeleton, which regulates cell shape and motility. Chemoattractant regulation of actin polymerization is a major event in remodeling of the cytoskeleton and the driving force behind directed cell movement (Condeelis *et al.,* 1988; Schmidt and Hall, 1998; Higgs and Pollard, 2001; Pollard and Borisy, 2003).

Many of the events underlying chemotaxis have been elucidated in the social amoebae *Dictyostelium discoideum* and in neutrophils (Zigmond, 1989; Parent and Devreotes, 1999; Rickert *et al.,* 2000; Chung *et al.,* 2001; Heit *et al.,* 2002; Wang *et al.,* 2002). Studies of these cells suggest that directional sensing is established by phosphatidyl-3′,4′,5′-triphosphate and/or phosphatidyl-3′,4′-bisphosphate [PI(3,4,5)P_3/PI(3,4)P_2] production and degradation at the plasma membrane in response to G-protein signaling. The levels of PI(3,4,5)P_3 are regulated by PI 3-kinases (PI3Ks) and the PI 3-phosphatase, PTEN (Buczynski *et al.,* 1997; Hirsch *et al.,* 2000; Li *et al.,* 2000; Sasaki *et al.,* 2000; Funamato *et al.,* 2001, 2002; Iijima and Devreotes, 2002; Stocker *et al.,* 2002). In resting *D. discoideum* cells, PI3Ks are found in the cytosol, whereas a fraction of PTEN is localized at the cell membrane. When cells are uniformly exposed to chemoattractant, the PI3Ks rapidly bind to the membrane and PTEN dissociates. As stimulation continues, the PI3Ks return to the cytosol, and PTEN reassociates with the membrane. When cells are exposed to a gradient of chemoattractant, PI3Ks and PTEN bind to the membrane at the front and rear of the cell, respectively. This leads to the selective accumulation of PI(3,4,5)P_3/PI(3,4)P_2 at the leading edge. Studies of *pten*$^-$ cells demonstrate a causal relationship between PI(3,4,5)P_3/PI(3,4)P_2 levels and actin polymerization. When exposed to a uniform stimulus, *pten*$^-$ cells exhibit a prolonged and stronger association of PH domain with the cell membrane and a parallel increase in actin polymerization. Placed in a chemoattractant gradient, *pten*$^-$ cells fail to produce sharp localizations of PI(3,4,5)P_3/PI(3,4)P_2 and F-actin at the cell's leading edge and chemotaxis is severely impaired (Funamato *et al.,* 2001; Iijima and Devreotes, 2002).

Although PI(3,4,5)P_3/PI(3,4)P_2 clearly regulates actin polymerization, polarity, and directional sensing, its essential function has been difficult to establish. Disruption of PI3K activity (deletion of two of three *D. discoideum* PI3Ks) impairs but does not block the ability of cells to sense and orient in chemotactic gradients (Buczynski *et al.,* 1997; Funamoto *et al.,* 2001). Similarly, disruption of mammalian PI3Ks and PTEN interfere with chemotaxis and motility, but the underlying biochemical mechanisms have not been defined. Also, PI3K inhibitors, LY294002 and wortmannin, have been reported to inhibit but do not prevent chemotaxis in a variety of cell types, unless unphysiologically high concentrations are used (Wu *et al.,* 2000; Wymann *et al.,* 2000; Wang *et al.,* 2002; unpublished observations). Moreover, mu-

Article published online ahead of print. Mol. Biol. Cell 10.1091/mbc.E03–05–0339. Article and publication date are available at www.molbiolcell.org/cgi/doi/10.1091/mbc.E03–05–0339.

* Corresponding author. E-mail address: pnd@jhmi.edu.

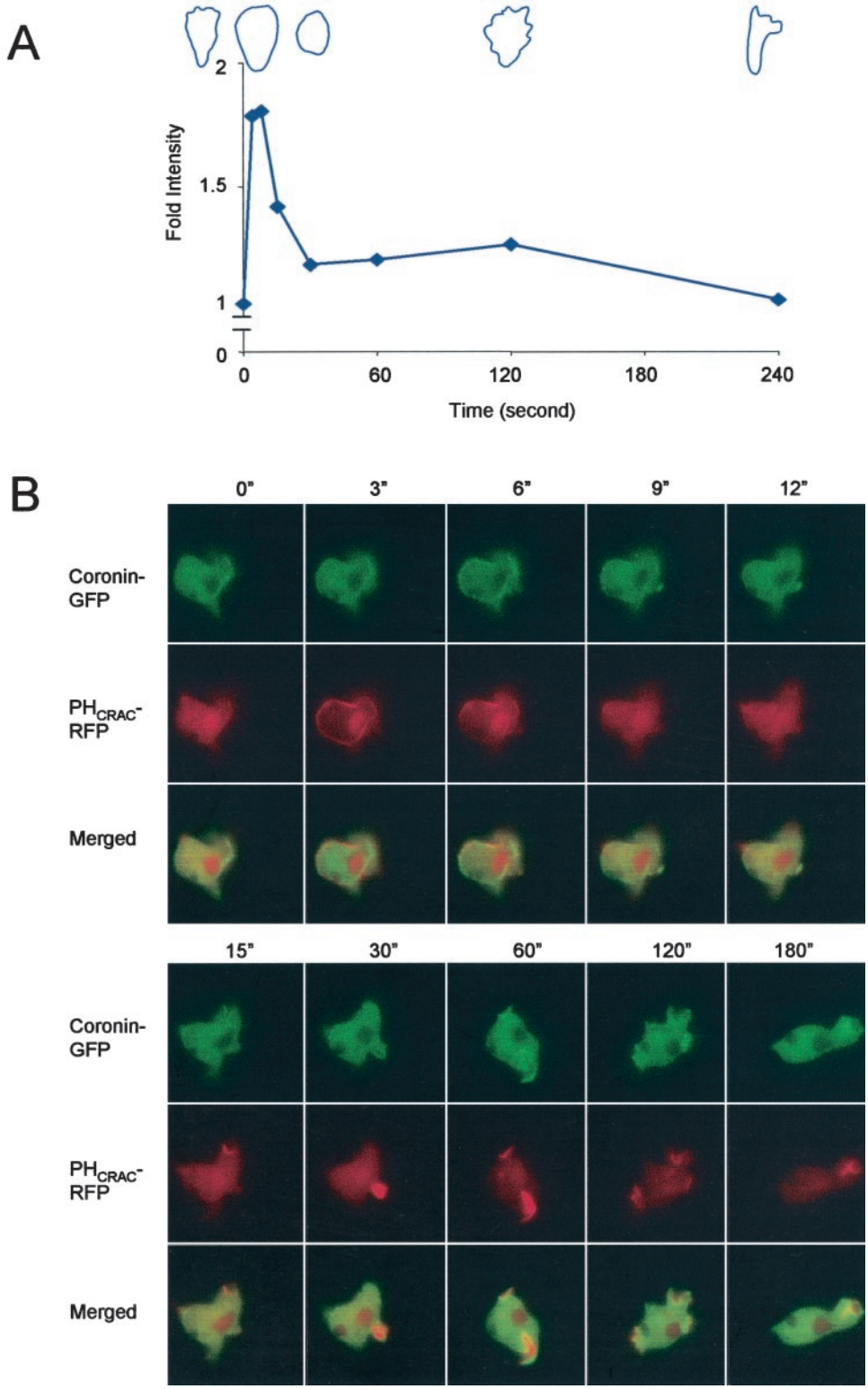

Figure 1. Assessment of actin dynamics in wild-type (WT) cells after a uniform cAMP stimulus. (A) Typical biphasic profile of actin polymerization assay from wild-type cells. All values were normalized to the amount of F-actin at time 0, which was taken just before addition of 1 μM cAMP. Typical cell shapes corresponding to time points are illustrated. (B) PH_{CRAC}-RFP and Coronin-GFP coexpressed WT cells were used to simultaneously monitor the localization of PI(3,4,5)P_3 and new F-actin in a living cell. Fluorescence images were captured at the indicated times after addition of 1 μM cAMP. (See video 1 in supplementary data.)

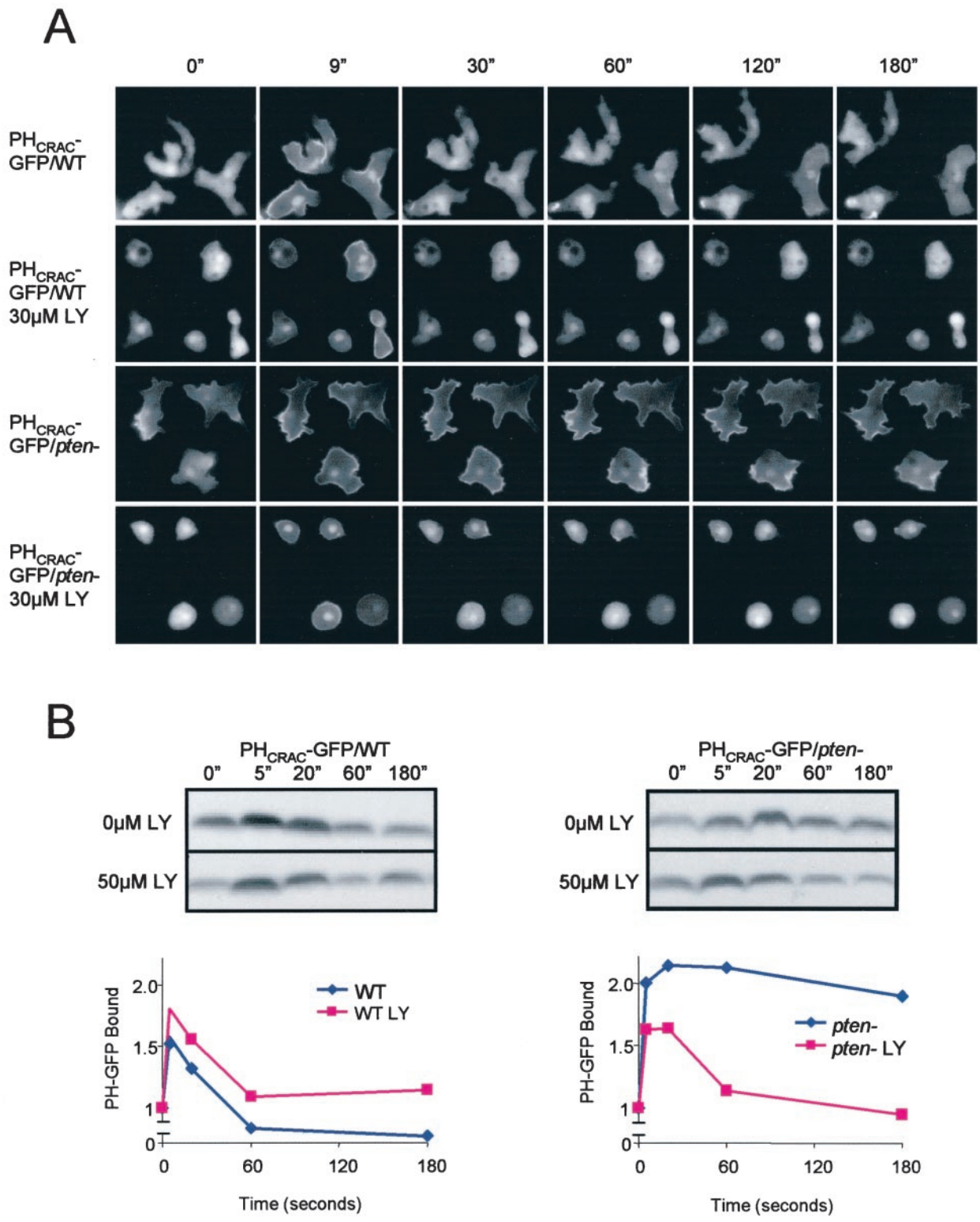

Figure 2. Monitoring PH_{CRAC}-GFP translocation in wild-type (WT) and *pten*$^-$ cells. (A) PH_{CRAC}-GFP expressed in WT and *pten*$^-$ cells was visualized by fluorescence microscopy. Images were captured at the indicated times after addition of 1 μM cAMP. When present, LY294002 was added 15 min before experiments. (See videos 2a–2d in supplementary data.) (B) PH_{CRAC}-GFP translocation assay in WT and *pten*$^-$ cells. Amount of membrane associated PH_{CRAC}-GFP in lysates prepared at times after addition of 1 μM cAMP was determined by immunoblot. Top: a typical immunoblot. Bottom: normalize data from two to four experiments.

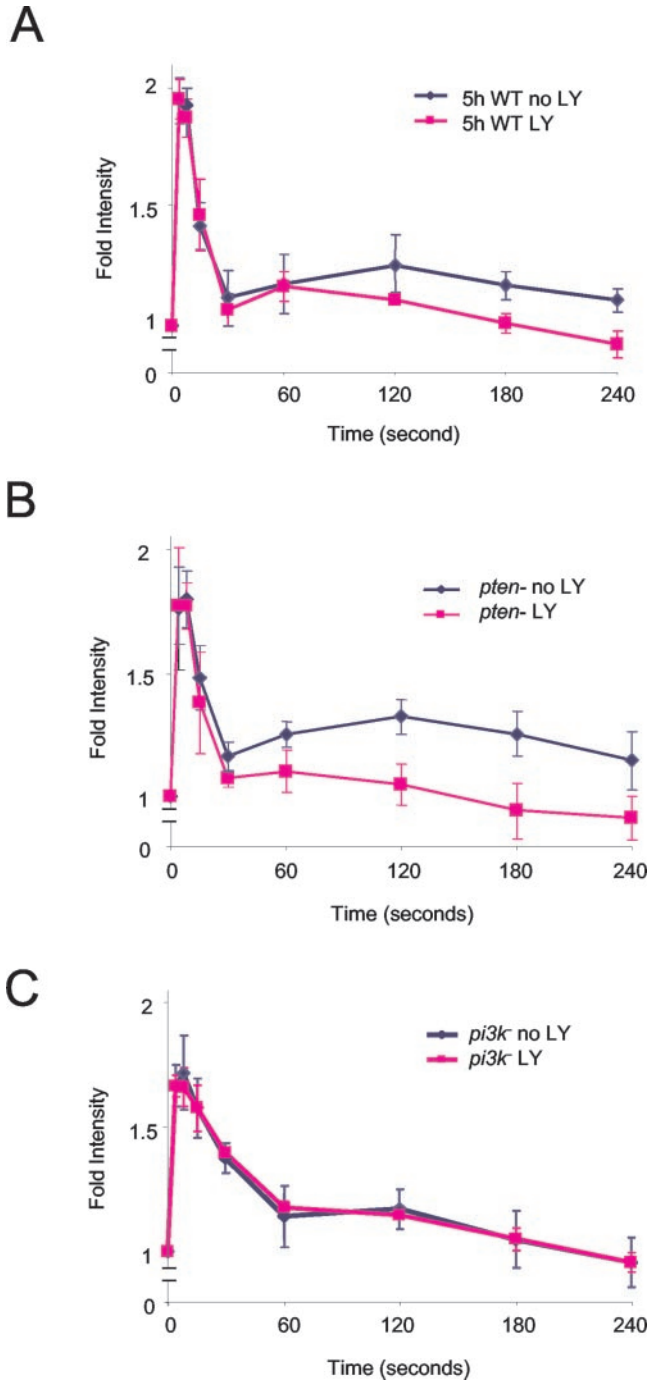

Figure 3. Actin polymerization assay in wild-type (WT), *pten*$^-$, and *pi3k1*$^-$/2$^-$ cells in the presence or absence of LY294002. Five-hour stage WT cells (A), *pten*$^-$ cells (B), and *pi3k1*$^-$/2$^-$ cells (C) were treated with 30 μM LY for 15 min before addition of 1 μM cAMP. Data shown are average of at least three independent experiments.

tations or inhibitors of PI3K do not significantly affect the rapid phase of chemoattractant-induced actin polymerization (Li *et al.*, 2000; Funamato *et al.*, 2001).

Previous studies analyzing actin polymerization in *D. discoideum* and neutrophils suggested the existence of a biphasic response to a uniform stimulus (Condeelis *et al.*, 1988; Norgauer *et al.*, 1994; Postma *et al.*, 2003). The cells undergo a series of discrete cell shape changes during the two phases of actin polymerization (Futrelle *et al.*, 1982; Condeelis *et al.*, 1990; Caterina and Devreotes, 1991; Chen *et al.*, 1996). During the first peak, cells freeze motion; then at ~30 s, as F-actin levels drop precipitously, cells round up or "cringe." During the second phase of actin polymerization, which lasts several minutes, the cells extend new pseudopods from multiple regions and start to move. Cells return to normal morphology shortly thereafter. Our data here shows that in *D. discoideum* the two phases of actin polymerization closely parallel a biphasic accumulation of PI(3,4,5)P_3/PI(3,4)P_2 and that the second phase of actin polymerization depends directly on the slow phase of PI(3,4,5)P_3 accumulation. We explore the role that each component of the biphasic responses has in directional sensing and during chemotaxis.

MATERIALS AND METHODS

Cell Culture and Development

D. discoideum cells were cultured in HL5 medium and developed for 5 h, unless otherwise indicated, in development buffer (DB buffer: 10 mM phosphate buffer, 2 mM $MgSO_4$, 0.2 mM $CaCl_2$) as previous described (Parent *et al.*, 1998). Cell lines used included wild-type cells (WT: AX2 or AX3); SCAR-GFP (from Dr. Saxe) expressed in AX2; PH_{CRAC}-GFP expressed in AX3; PH_{CRAC}-RFP and Coronin-GFP (from Dr. Gerisch) expressed in AX3; and *pi3k1*$^-$/*pi3k2*$^-$ (*pi3k1*$^-$/2$^-$, from Dr. Firtel), *pten*$^-$, and PH_{CRAC}-GFP expressed in *pten*$^-$.

Actin Polymerization Assay

Actin polymerization assays were carried out as previously described (Iijima and Devreotes, 2002; Zigmond *et al.*, 1997). To achieve a basal level, developed cells were shaken at 200 rpm with 2 mM caffeine in PM buffer for 30 min, collected, washed, resuspended at 3×10^7/ml with 2 mM caffeine in PM buffer (10 mM phosphate buffer, 2 mM $MgSO_4$), and shaken at room temperature for no more than 30 min. At various time points after adding 1 μM cAMP, aliquots of cells were taken, fixed, and stained with TRITC-phalloidin. (Buffer for fix and stain: 3.7% formaldehyde, 0.1% Triton, 250 nM TRITC-Phalloidin, 20 mM KPO_4, 10 mM PIPES, 5 mM EGTA, 2 mM $MgCl_2$, pH 6.8). F-actin was proportional to the amount of phalloidin fluorescence (Excitation wavelength: 540 nm. Emission wavelength: 570 nm.) extracted from cell pellets.

Immunoblot Analysis of PH Domain Translocation

The assay was performed as described (Parent *et al.*, 1998). Cells were pretreated with caffeine, then washed, and resuspended in PM buffer at 8×10^7/ml. At indicated time points after stimulation with 1 μM cAMP, fractions of cells were filter-lysed into ice-cold PM buffer to terminate the reaction. Membrane fractions were collected and assayed by immunoblot of PH_{CRAC}-GFP with anti-GFP antibody.

Fluorescence Microscope

Images of living cells were observed using Zeiss inverted microscopes (Axiovert 135TV and Axiovert 100; Zeiss, Oberkochen, Germany) as previous described (Parent *et al.*, 1998). Cells were allowed to adhere on a chamber (Lab-tek, Nalge Nunc, Rochester, NY) and stimulated by 1 μM cAMP. To image double-labeled cells, filter wheels carrying the exciters HQ480/25 and D565/25 were used along with the emitters HQ525/40 and D620/60 (filters from Chroma, Rockingham, VT). IP lab and Image J (Scanalytics, Fairfax, VA) software packages were used to collect and process data.

Chemotaxis Assay and Quantification

Chemotactic movements of cells to a micropipette containing cAMP were performed as described (Parent *et al.*, 1998). Cells were allowed to adhere on a chambered coverglass (Lab-tek, Nalge Nunc). A micropipette filled with 10 μM cAMP was positioned, and images of moving cells were recorded. IP lab and Image J software packages were used to collect and process data.

Speed of chemotaxis was calculated from the distance a cell covered divided by the time. Chemotactic Index was defined as the cosine of the angle formed by the line between the cell start point and the micropipette tip point and the line from the cell start point to the cell ending point (Iijima and Devreotes, 2002). Speed and Chemotactic index were measured during a period of 200 s.

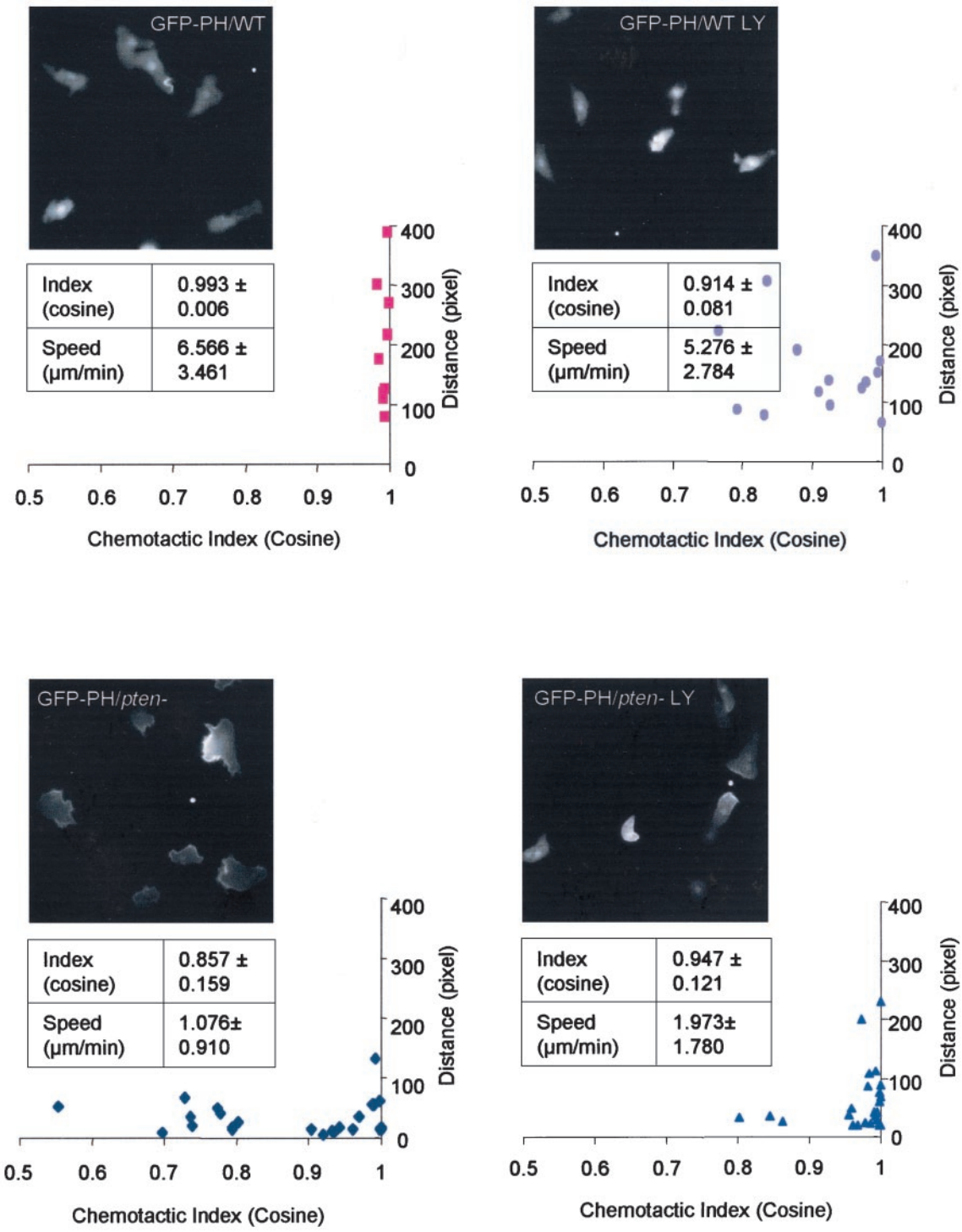

Figure 4. Chemotaxis to a micropipette filled with 10 μM cAMP. Fluorescent microscopic images of wild-type (WT) and *pten*$^-$ cells expressing PH_{CRAC}-GFP in the presence or absence of 30 uM LY were taken at 10-s interval for 10 min. Frames demonstrate typical cell shape and PH_{CRAC}-GFP localization for each condition. White spot indicates the location of the micropipette. (See videos 4a–4d in supplementary data.) Average speed and chemotactic index were calculated from at least three independent experiments. Distribution of the speed (presented as pixels covered in 10 min) and chemotactic index of cells were also calculated and plotted.

RESULTS

Previous studies of actin polymerization suggested the existence of a biphasic response to a uniform cAMP stimulus. When we stimulated optimally differentiated 5-h stage cells, we observed a clear biphasic response. The first phase comprised a twofold increase over the basal level, which peaked within seconds after the addition of cAMP and ended by

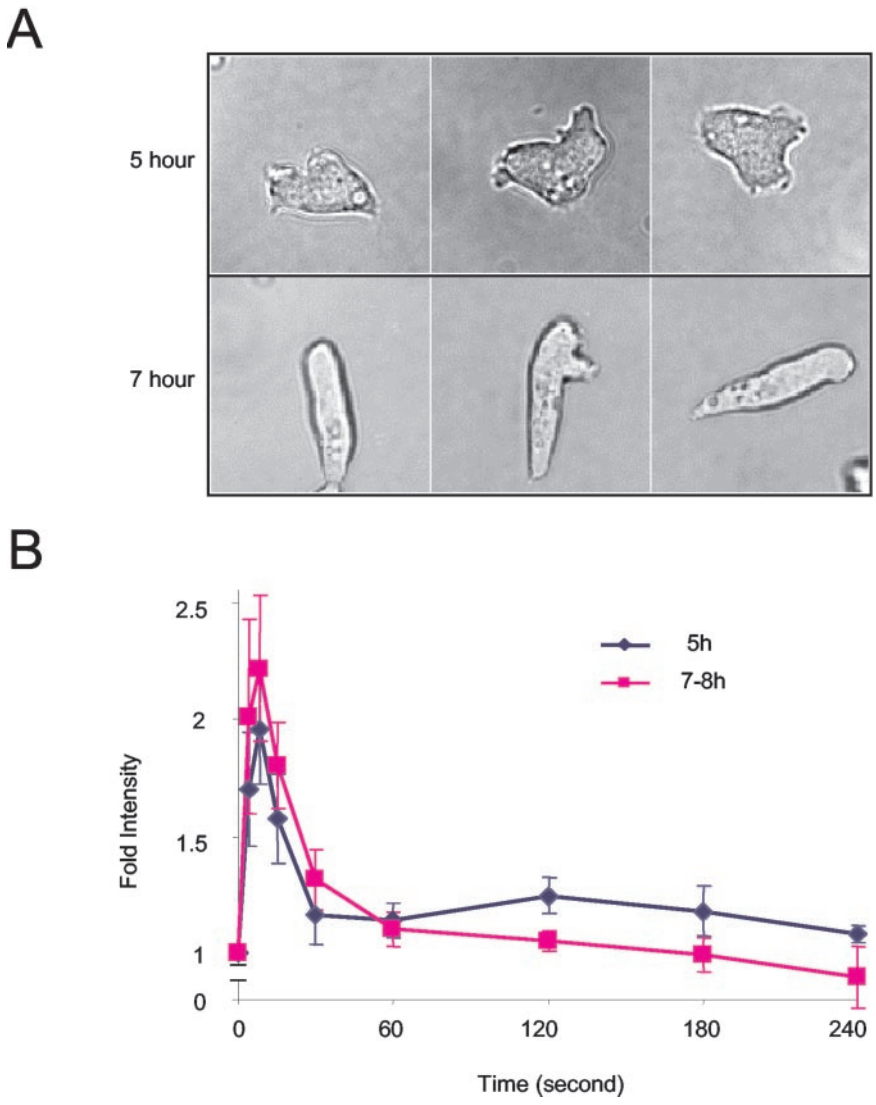

Figure 5. Comparison of cell morphology and biphasic actin response at different stages of development. (A) Wild-type (WT) cells chemotaxing in cAMP gradients. Typical examples of cells at 5- and 7-h stage are shown. (B) Actin polymerization assay in 5- and 7-h stage WT cells. Data shown are average of five independent experiments.

30 s. The second phase was smaller, usually less than a 25% increase and occurred between 60 and 180 s (Figure 1A). To elucidate the relationship of PI(3,4,5)P_3/PI(3,4)P_2 and actin polymerization, we cotransformed PH_{CRAC}-RFP and coronin-GFP into WT cells. Like some other PH-domains, evidence strongly suggests that the translocation of the PH_{CRAC} domain to the membrane reflects the local PI(3,4,5)P_3/PI(3,4)P_2 accumulation (Iijima and Devreotes, 2002; Huang *et al.*, 2003; Lemmon, 2003). To assess actin dynamics in living cells, we followed the movement of coronin-GFP to the cortex. Coronin is known to localize with newly formed F-actin and has been suggested to bind to the Arp2/3 complex (de Hostos, 1999; Mishima and Nishida, 1999; Humphries *et al.*, 2002). In response to a uniform stimulus, both proteins displayed two phases of association to the cell perimeter. Within seconds, PH_{CRAC}-RFP was recruited uniformly to the cell membrane. It then returned to the cytosol and a second phase, localized to membrane extensions, ensued (Figure 1B, red). The two phases of PH_{CRAC} translocation have also been observed by Postma *et al.* (personal communication). For coronin-GFP, the first translocation was uniformly localized at the cell cortex, whereas the second was localized to regions of newly formed pseudopods (Figure 1B, green). The spatial and temporal features of each response were similar, but the PH_{CRAC}-RFP recruitment to the membrane appeared to precede association of coronin-GFP with the cortex. However, increased temporal resolution will be required to verify this point. The PH_{CRAC}-RFP clearly localized more peripherally than coronin-GFP (Figure 1B, merged). We observed similar biphasic membrane recruitments with another actin-binding protein, SCAR (from Dr. Saxe, Bear *et al.*, 1998) and also with PI3K2 (unpublished data).

We examined the biphasic response in WT and *pten*$^-$ cells in the absence or presence of the PI3K inhibitor LY294002 (LY). PH_{CRAC}-GFP was used as a marker for PI(3,4,5)P_3/PI(3,4)P_2 accumulation. As previously reported, levels of PI(3,4,5)P_3/PI(3,4)P_2 production and actin polymerization were significantly larger during the period from 30 to 180 s in the *pten*$^-$ cells (Figure 2, A and B). The first peak recruited PH_{CRAC}-GFP uniformly to the cell perimeter. During the large second phase in the *pten*$^-$ cells, PH_{CRAC}-GFP bound to the membrane at the points where cells were spreading. Addition of 30 μM LY caused a rounding and a reduction of the membrane ruffles in both WT cells and *pten*$^-$ cells (Figure 2A). When these treated cells were stimulated, the sec-

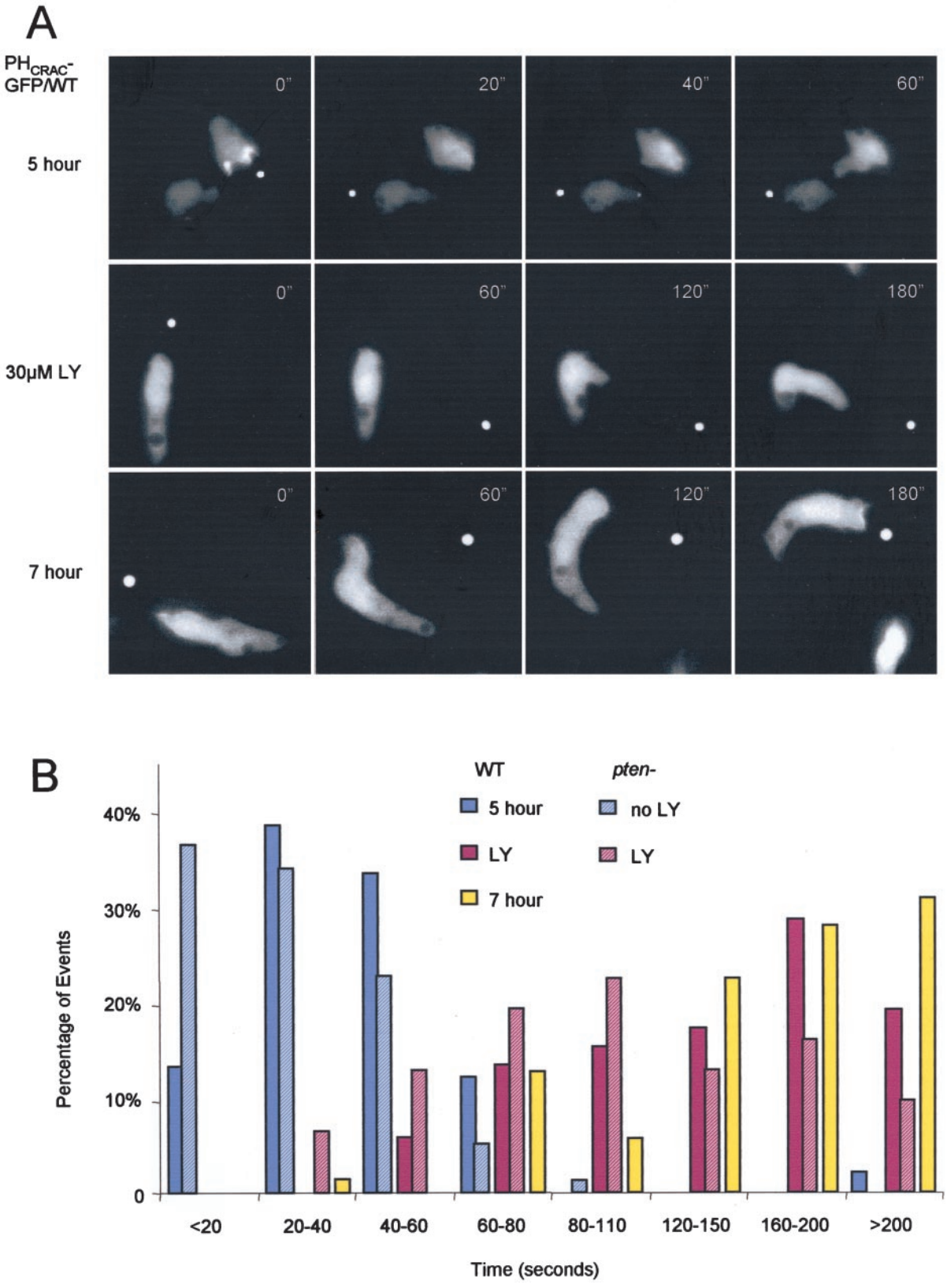
A
PH$_{CRAC}$-GFP/WT
5 hour
30μM LY
7 hour
0"
20"
40"
60"
120"
180"
B
WT
pten-
5 hour
LY
7 hour
no LY
LY
40%
30%
20%
10%
0
Percentage of Events
<20
20-40
40-60
60-80
80-110
120-150
160-200
>200
Time (seconds)

Figure 6.

ond phase of PH_{CRAC}-GFP translocation was selectively inhibited. In both cell types treated with LY, the first peak of chemoattractant-induced PH_{CRAC}-GFP translocation was still detectable by microscopy and by immunoblot (Figure 2B).

With these observations in hand, we reexamined actin polymerization using PI3K inhibitors as well as *pi3k1*$^-$/2$^-$ and *pten*$^-$ cells. In WT cells, 30 μM LY blocked the second phase of actin polymerization with little effect on the initial rapid phase (Figure 3A). In *pten*$^-$ cells, the enlarged second phase of actin polymerization was selectively inhibited with 30 μM LY or 10 μM wortmannin, another PI3K inhibitor (Figure 3B and unpublished data). Inhibition of the first and second phases of actin polymerization by 30 μM LY in *pten*$^-$ cells were 0 and >85%, respectively. In the *pi3k1*$^-$/2$^-$ cells, there was no obvious second phase and the first phase was insensitive to 30 μM LY (Figure 3C). Higher concentrations of LY than those used in Figure 2 (up to 200 μM) did eventually inhibit the rapid phase of PI(3,4,5)P_3/PI(3,4)P_2 production. Curiously, these high concentrations, which are likely unphysiological, elevated basal F-actin levels to those normally found at the peak of the rapid phase. Under these conditions, there was little further increase induced by chemoattractant (unpublished data).

We next examined directed movements of WT and *pten*$^-$ cells treated with 30 μM LY. Addition of the drug, which blocked the second phase of the response to a uniform stimulus, impaired chemotaxis of WT cells. In the absence of LY, the cells moved randomly until exposed to a gradient and then moved toward the micropipette by turning or creating new leading edges. With LY treatment, random movement and membrane ruffles were significantly reduced. When the gradient was applied, the cells polarized and moved toward the chemoattractant, although they moved more slowly and displayed fewer lateral pseudopods. PH_{CRAC}-GFP was detected less often along the leading edge of the treated cells compared with WT cells (Figure 4, top). As previously described, most *pten*$^-$ cells are defective in speed and directional sensing, although there is a subset of *pten*$^-$ cells that displays nearly normal chemotactic indices. Interestingly, although LY impaired chemotaxis of the WT cells, it actually improved the chemotactic responses of *pten*$^-$ cells (Figure 4, bottom). The PH_{CRAC}-GFP staining was more localized, and the cells acquired a narrower leading edge, extended fewer lateral pseudopods, and moved rapidly toward chemoattractant (Figure 4, bottom). For each experimental condition, we quantified the speed and chemotactic index from three sets of independent experiments (Figure 4). Although LY treatment reduced the average speed of WT cells ~20%, it increased that of the *pten*$^-$ cells by about twofold. Also, the drug decreased the chemotactic index of WT cells but increased that of the *pten*$^-$ cells. Thus, the second phases of the PI(3,4,5)P_3 accumulation and actin polymerization are tightly regulated by PI3K, and optimal levels are required for efficient directed movement. However, cells substantially lacking the second phases or with elevated second phases were still able, albeit inefficiently, to chemotax.

The two phases of PI(3,4,5)P_3 accumulation and actin polymerization were next examined at different stages of development. Under starvation conditions, *D. discoideum* cells undergo differentiation and become polarized. Growth phase cells are unpolarized and project many lateral pseudopods. As cells differentiate, polarity increases; 7-h stage cells are elongated and maintain a persistent leading edge (Figure 5A). Cells grown in the presence of bacteria, which are quite unpolarized, displayed a second phase of actin polymerization when stimulated with folic acid (unpublished data). In 5-h stage cells, which are relatively unpolarized, we also observed a significant second peak of PI(3,4,5)P_3/PI(3,4)P_2 and actin polymerization (Figures 1, 2, and 5B). In 7-h polarized cells, the second phases of cell spreading and PH_{CRAC}-GFP translocation were less apparent by microscopy. Similarly, when we examined actin polymerization in 7-h cells, the second phase was significantly reduced (Figure 5).

Careful examination suggested that the second phase of the response determined the cell's capacity to extend lateral pseudopods in the new direction when the gradient was switched. In 5-h stage cells the leading edge is less defined and is not persistently maintained during movement. By comparison, the 7-h stage cells are polarized and normally turn when changing directions, as occurs when a micropipette containing cAMP is moved to a new location. To quantitate these behaviors, we repeatedly moved a micropipette tip and recorded the time (referred to as "delay time") for the leading edge of the cell to display sustained movement in the new direction. Figure 6A shows examples of this behavior, and data from many events are shown in Figure 6B. For the 5-h cells, the average "delay time" was 48 s and 90% of the events occurred within 1 min. LY treatment of these cells increased the average "delay time" to 146 s. This was similar to that of 7-h cells, where the average "delay time" was 162 s. Interestingly, the *pten*$^-$ cells had a short "delay time" (average 37 s) and often extended lateral pseudopods spontaneously. Treatment of the *pten*$^-$ cells with 30 μM LY increased the "delay time" (average 114 s) toward the WT cell level (Figure 6B). Although the "delay times" of the 5-h cells and *pten*$^-$ cells treated with LY were both similar to the 7-h cells, the treated *pten*$^-$ cells displayed a more normal morphology and behavior (unpublished data).

Figure 6 (facing page). Analysis of wild-type (WT) cells at the 5-h stage in the absence and presence of LY and at the 7-h stage switching directions after micropipette repositioning. (A) Fluorescent images of cells switching direction in response to new cAMP gradient. Relative times between frames are indicated on images. (See videos 6a–6c in supplementary data.) (B) Quantification of the "delay time" required for switching direction. Time between frames was 10 s. The time required for the leading edge to display sustained movement for two continuous frames toward the micropipette was determined. Number of events were binned in 20-s intervals and plotted as a histogram. One direction switch was considered one event. Five independent experiments (22 cells, 98 events) were quantified for 5-h stage WT cells. Seven independent experiments were quantified for both 30 μM LY-treated WT cells (22 cells, 41 events) and 7-h stage WT cells (30 cells, 63 events). Three independent experiments were quantified for both *pten*$^-$ (11 cells and 79 events) and *pten*$^-$ plus LY (19 cells and 31 events).

DISCUSSION

Our observations indicate an intimate connection between the spatial and temporal regulation of PI(3,4,5)P_3 accumulation and actin polymerization. Chemoattractants trigger biphasic changes in each response. The first phase is rapid and uniformly localized around the cell perimeter. Concomitantly, the cells freeze and round up. The second phase is slower and is localized to regions of the periphery, corresponding to cellular extensions. Inhibition of PI3K selectively abrogates, whereas disruption of PTEN enhances the second phase of PI(3,4,5)P_3 accumulation. These perturba-

tions cause parallel changes in the second phase of actin polymerization. The slow phase of actin polymerization triggered by a uniform temporal stimulus correlates with the capacity of the cells to extend lateral pseudopods when the direction of a chemotactic gradient is switched. Proper chemotactic movement appears to depend on an optimal level of the second phase of the response and a corresponding capacity for lateral pseudopod extension. Thus, the inhibition of PI3K impairs chemotaxis in WT cells but actually improves chemotaxis in the *pten*$^-$ cells.

Local accumulations of PI(3,4,5)P_3 appear to control many actin based cellular extensions including the spontaneous ruffles that occur during random migration as well as the second phase of the chemoattractant-induced response. LY-treated cells display very few membrane ruffles, and pseudopods are mainly distributed at the side of the cell facing the high concentration of chemoattractant. When direction of the gradient is switched, the treated cells display some of the characteristics of more polarized cells. For example, the "delay time" increases substantially upon a gradient switch. It approaches the longer "delay time" of the 7-h cells, which must turn to seek the new gradient. The "delay time" is shorter in 5-h cells because they are able to extend lateral pseudopods and create a new front. Furthermore, *pten*$^-$ cells, which have a very large second phase, are unpolarized, switch fronts rapidly, and have increased spontaneous ruffle activity.

It is unclear why an optimal level of second phase response, which allows cells to rapidly react to a switch in gradient direction, improves the chemotactic response to a stable gradient. We speculate that cells that are unable to react rapidly to gradient shifts may be slow to "correct" their direction if they get "off tract." This deficiency might lead to inefficient directional migration. On the other hand, excess second phase response as occurs in *pten*$^-$ cells also leads to inefficient chemotaxis. In growing cells, which must track motile bacteria and 5-h stage cells, which have not yet been recruited to a specific group of streaming cells, the ability to switch direction easily is advantageous. The second phase of the actin response decreases as cell polarity increases, and most cells have already formed streams during aggregation. This may allow cells to move more rapidly when switching direction is less critical.

The significance of the two phases of actin polymerization has not been fully appreciated, perhaps because the phenomenon has not been consistently observed. In fact, it is difficult to observe unless conditions are carefully controlled. Even in the absence of a stimulus, cells move randomly, making pseudopods and ruffles that contribute to the basal level of filamentous actin. With a uniform stimulus, cells respond synchronously during the first peak, but individual cells generate new extensions and ruffles asynchronously during the second phase (Figures 1B and 2A). These tend to average out and lower the apparent level of the response. In 7-h developed cells, the frequency or intensity of ruffling during the second phase never exceeds that present before the stimulus and thus the second peak of actin polymerization is undetectable.

We are puzzled that the first phase of PI(3,4,5)P_3 accumulation is relatively insensitive to PI3K inhibitors. One might speculate that transient loss of PTEN from the membrane contributes to the first phase of PI(3,4,5)P_3 production. That is, even when PI3K is quite inhibited, the chemoattractant-induced decrease of PTEN activity is significant enough to elevate PI(3,4,5)P_3 levels. However, we ruled out this possibility, because LY treatment does not inhibit the first phase even in *pten*$^-$ cells. The fact that LY inhibits the second peak also indicates that the drug enters the cell efficiently. Once again, it is not clear why the first peak is not inhibited. It is possible that there is an inhibitor-resistant PI3K activity or it may be the drug cannot access the PI3K during the initial phase.

Our results clearly show that the second phase of actin polymerization is controlled directly by the production of PI(3,4,5)P_3. But the question remain as to whether PI(3,4,5)P_3 is essential for the first peak of actin polymerization. In our experiments, the LY concentration used (30 μM or 50 μM) did not fully inhibit the first phase of PH_{CRAC}-GFP translocation. Therefore, we cannot conclude whether PI(3,4,5)P_3 is required for this rapid burst of actin polymerization. Unphysiologically high drug concentrations did substantially decrease the first phase of PI(3,4,5)P_3 accumulation. However, the first peak of actin polymerization was impossible to assess because basal levels of F-actin increased substantially. Interestingly, the first peak of actin polymerization was also unaffected in *pi3k1*$^-$*/2*$^-$ cells, which retain only 10–15% of the WT level of chemoattractant-induced PI(3,4,5)P_3 accumulation (Huang *et al.*, 2003). It may be that very few PI(3,4,5)P_3 molecules can trigger actin polymerization and there are further amplification steps downstream of PI(3,4,5)P_3 production.

Alternatively, a redundant pathway downstream of the G-proteins may control the first peak of actin polymerization. We are currently exploring the conditions that can fully block the rapid response to chemoattractant. It has been suggested that PLC activation and a consequent decrease in PI(4,5)P_2 could contribute to the first phase of actin polymerization in mammary carcinoma cells stimulated with EGF (Condeelis, personal communication). We tested this mechanism in *D. discoideum* by monitoring the chemoattractant-induced actin response in *plc*$^-$ cells (from Dr. Van Haastert) treated with LY. The first peak of the actin polymerization was unaffected under these conditions. Current efforts are focused on other possible intermediates that may directly contribute to the first phase of actin polymerization.

ACKNOWLEDGMENTS

Several plasmids were generous gifts from different laboratories: monomeric RFP, Roger Tsien; GFP-labeled SCAR, Dr. Saxe; and Coronin-GFP, Dr. Gerisch. Cell lines *plc*$^-$ and *pi3k1*$^-$*/pi3k2* were generous gifts from Dr. Van Haastert and Dr. Firtel, respectively. This research was supported by Public Health Service Grants 28007 and 34933 to P.N.D. and an American Cancer Society Fellowship to C.J.

REFERENCES

Bear, J.E., Rawls, J.F., and Saxe, C. L., III. (1998). SCAR, a WASP-related protein, isolated as a suppressor of receptor defects in late *Dictyosteium* development. J. Cell Biol. *142,* 1325–1335.

Buczynski, G., Grove, B., Nomura, A., Kleve, M., Bush, J., Firtel, R.A., and Cardelli, J. (1997). Inactivation of two *Dictyostelium discoideum* genes, DdPIK1 and DdPIK2, encoding proteins related to mammalian phosphatidylinositide 3-kinases, results in defects in endocytosis, lysosome to postlysosome transport, and actin cytoskeleton organization. J. Cell Biol. *136,* 1271–1286.

Caterina, M.J., and Devreotes, P.N. (1991). Molecular insights into eukaryotic chemotaxis. FASEB J. *15,* 3078–3085.

Chen, M.Y., Install, R.H., and Devreotes, P.N. (1996). Signaling through chemoattractant receptors in *Dictyostelium.* Trend Genet. *12,* 52–57.

Chung, C.Y., Funamoto, S., and Firtel, R.A. (2001). Signaling pathways controlling cell polarity and chemotaxis. Trends Biochem. Sci. *26,* 557–566.

Condeelis, J., Bresnick, A., Demma, M., Dharmawardhane, S., Eddy, R., Hall, A.L., Sauterer, R., and Warren, V. (1990). Mechanisms of amoeboid chemotaxis: an evaluation of the cortical expansion model. Dev. Genet. *11,* 333–340.

Condeelis, J., Hall, A., Bresnick, A., Warren, V., Hock, R., Bennett, H., and Ogihara, S. (1988). Actin polymerization and pseudopod extension during amoeboid chemotaxis. Cell Motil. Cytoskel. *10,* 77–90.

de Hostos, E.L. (1999). The coronin family of actin-associated proteins. Trends Cell Biol. *9,* 345–350.

Funamoto, S., Milan, K., Meili, R., and Firtel, R.A. (2001). Role of phosphatidylinositol 3′ kinase and a downstream pleckstrin homology domain-containing protein in controlling chemotaxis in *Dictyostelium.* J. Cell Biol. *153,* 795–810.

Funamoto, S., Meili, R., Lee, S., Parry, L., and Firtel, R.A. (2002). Spatial and temporal regulation of 3-phosphoinositides by PI 3-kinase and PTEN mediates chemotaxis. Cell *109,* 611–623.

Futrelle, R.P., Traut, J., and McKee, W.G. (1982). Cell behavior in *Dictyostelium discoideum*: preaggregation response to localized cyclic AMP pulses. J. Cell Biol. *92,* 807–821.

Heit, B., Tavener, S., Raharjo, E., and Kubes, P. (2002). An intracellular signaling hierarchy determines direction of migration in opposing chemotactic gradients. J. Cell Biol. *159,* 91–102.

Higgs, H.N., and Pollard, T.D. (2001). Regulation of actin filament network formation through ARP2/3 complex: activation by a diverse array of proteins. Annu. Rev. Biochem. *70,* 649–676.

Hirsch, E. *et al.* (2000). Central role for G protein-coupled phosphoinositide 3-kinase gamma in inflammation. Science, *287,* 1049–1053.

Huang, Y.E., Iijima, M., and Devreotes, P.N. (2003). Receptor mediated regulation of PI3Ks confines PI(3, 4, 5)P_3 to the leading edge of chemotaxing cells. Mol. Biol. Cell *14,* 1913–1922.

Humphries, C.L., Balcer, H.I., D'Agostino, J.L., Winsor, B., Drubin, D.G., Barnes, G., Andrews, B.J., and Goode, B.L. (2002). Direct regulation of Arp2/3 complex activity and function by the actin binding protein coronin. J. Cell Biol. *159,* 993–1004.

Iijima, M., and Devreotes, P.N. (2002). Tumor suppressor PTEN mediates sensing of chemoattractant gradients. Cell *109,* 599–610.

Lemmon, M.A. (2003). Phosphoinositide recognition domains. Traffic *4,* 201–213.

Li, Z., Jiang, H., Xie, W., Zhang, Z., Smrcka, A.V., and Wu, D. (2000). Roles of PLC-β2 and -β3 and PI3Kγ in chemoattractant-mediated signal transduction. Science *287,* 1046–1049.

Mishima, M., and Nishida, E. (1999). Coronin localizes to leading edges and is involved in cell spreading and lamellipodium extension in vertebrate cells. J. Cell Sci. *112,* 2833–2842.

Norgauer, J., Krutmann, J., Dobos, G.J., Traynor-Kaplan, A.E., Oades, Z.G., and Schraufstatter, I.U. (1994). Actin polymerization, calcium-transients, and phospholipid metabolism in human neutrophils after stimulation with interleukin-8 and N-form peptide. J. Invest. Dermatol. *102,* 310–314.

Parent, C.A., Blacklock, B.J., Froehlich, W.M., Murphy, D.B., and Devreotes, P.N. (1998). G protein signaling events are activated at the leading edge of chemotactic cells. Cell *95,* 81–91.

Parent, C.A., and Devreotes, P.N. (1999). A cell's sense of direction. Science *284,* 765–770.

Pollard, T.D., and Borisy, G.G. (2003). Cellular motility driven by assembly and disassembly of actin filaments. Cell *112,* 453–465.

Postma, M., Roelofs, J., Goedhart, J., Gadella, T.W.J., Visser, A.J.W.G. and Van Haastert, P.J.M. Uniform cAMP stimulation of *Dictyostelium* cells induces localized patches of signal transduction and pseudopodia. *14,* 000–000.

Rickert, P., Weiner, O.D., Wang, F., Boune, H.R., and Servant, G. (2000). Leukocytes navigate by compass: role of PI3Kγ and its lipid products. Trends Cell Biol. *10,* 466–473.

Sasaki, T. *et al.* (2000). Function of PI3Kgamma in thymocyte development, T cell activation, and neutrophil migration. Science *287,* 1040–1046.

Schmidt, A., and Hall, M.N. (1998). Signaling to the actin cytoskeleton. Annu. Rev. Cell Dev. Biol. *14,* 305–338.

Stocker, H., Andjelkovic, M., Oldham, S., Laffargue, M., Wymann, M.P., Hemmings, B.A., and Hafen, E. (2002). Living with lethal PIP3 levels: viability of flies lacking PTEN restored by a PH domain mutation in Akt/PKB. Science *295,* 2088–2091.

Wang, F., Herzmark, P., Weiner, O.D., Srinivasan, S., Servant, G., and Bourne, H.R. (2002). Lipid products of PI(3)Ks maintain persistent cell polarity and directed motility in neutrophils. Nat. Cell Biol. *4,* 513–518.

Wu, D., Huang, C.K., and Jiang, H. (2000). Roles of phospholipid signaling in chemoattractant-induced responses. J. Cell Sci. *113,* 2935–2940.

Wymann, M.P., Sozzani, S., Altruda, F., Mantovani, A., and Hirsch, E. (2000). Lipids on the move: phosphoinositide 3-kinases in leukocyte function. Immunol. Today *21,* 260–264.

Zigmond, S.H. (1989). Chemotactic response of neutrophils. Am. J. Cell Mol. Biol. *1,* 451–453.

Zigmond, S.H., Joyce, M., Borleis, J., Bokoch, G.M., and Devreotes, P.N. (1997). Regulation of actin polymerization in cell-free systems by GTPγS and CDC42. J. Cell Biol. *138,* 363–374.